研 究 速 報

Model Tests on Seismic Behavior of Soil Retaining Walls

土留め擁壁の地震時挙動に関する模型実験

Yulman MUNAF*, Junichi KOSEKI* and Takeshi SATO*

ユールマン ムナフ・古 関 潤 一・佐 藤 剛 司

INTRODUCTION

In seismic design of soil retaining structures in Japan, the earth pressure acting on the wall has been traditionally evaluated based on the Mononobe-Okabe theory[1], which has also been most widely accepted in the world[2]. Essentially the Mononobe-Okabe theory is based on a pseudo-static limit-equilibrium type approach, which was derived from Coulomb theory by adding the effect of inertia forces due to earthquake on the potential soil wedge.

On the other hand, other theoretical analyses have been conducted by previous researchers. By conducting the sliding block analysis originally developed by Newmark[3], Richard and Elms[4] proposed an alternative design procedure which is based on the concept of limited displacement. Finite element method was adopted by Nadim and Whitman[5], and finite difference method by Siddarthan et. al.[6].

As for case histories, failure of several retaining walls during the 1995 Hyogoken-Nambu Earthquake has been reported by Tatsuoka, et. al.[7], and preliminary analyses on these walls by using current design method have been reported by Koseki, et. al.[8].

Furthermore, a variety of experimental studies have been performed to investigate seismic behavior of soil retaining walls. However, their failure mechanism has not yet been fully understood. Therefore, a series of pseudo-static model tests (tilting tests) have been planned in this study, and part of them have been conducted.

* Dept. of Building and Civil Engineering, Institute of Industrial Science, University of Tokyo

EQUIPMENT AND SOIL PROPERTIES

Fig. 1 shows the general view of the small apparatus which consists of: (1) a sand box; (2) a tilting equipment (hydraulic jack); (3) a model retaining wall and sand layers; and (4) a data acquisition system. The sand box is 100 cm long, 30 cm high and 10 cm wide, which is made of a rigid steel at the bottom side and acrylic transparent plates in the side walls. Facing of the model retaining wall is made of steel plate covered by smooth plastic to make a smooth contact with sand, and it is connected by hinge to the bottom side of sand box. To measure vertical force and horizontal force acting on the facing, one unit of two-component load cell (Bs and Bp) was installed at the toe of facing, and another normal load cell (A) was connected by a movable steel rod to the top of the facing. To reduce friction at the connecting point between facing and the movable steel rod, a roll bearing was used. A displacement transducer was set at the top of the facing to measure lateral displacement.

Fig. 2 shows a schematic cross section of the large

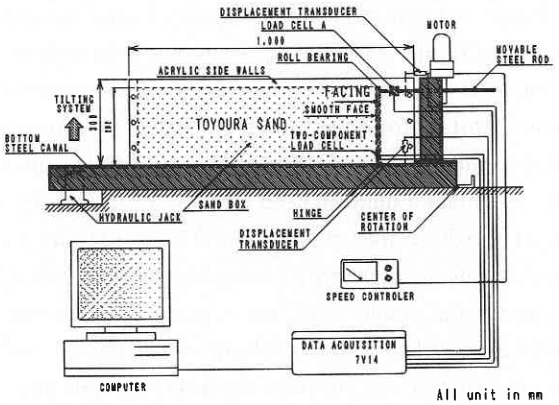

Fig. 1 General View of Small Apparatus

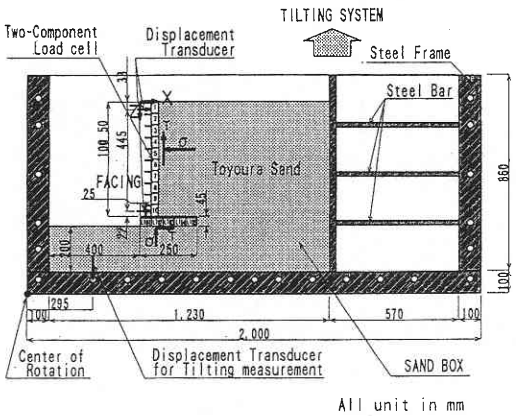

Fig. 2 Experimental Set-up of Large Apparatus

apparatus which consists of: (1) a sand box; (2) a tilting system; (3) a model retaining wall and sand layers. The sand box has inside dimensions of 180 cm long, 86 cm high and 60 cm wide, and it is made of a rigid steel frame and acrylic transparent plates in the side walls. Facing and bottom part of the model retaining wall are made of wooden blocks reinforced with steel bars ϕ=10 mm. Their surfaces are covered with sand paper to obtain rough contact with sand. To measure the distribution of normal stress σ and shear stress τ, fifteen units of two-component load cells, as used by Tateyama[9], were installed in the center part of the facing and the bottom of the wall. Two displacement transducers were set at the facing and one at the bottom to measure displacement and rotation of the wall. In both apparatus, Toyoura sand was used as back fill and subsoil layers, which has e_{max}=0.977; e_{min}=0.605; G_s=2.64; D_{10}=0.11 mm and D_{50}=0.16 mm.

TESTING PROCEDURES

The testing procedures using the small apparatus consist of 3 steps; (1) filling of sand; (2) tilting of sand box and (3) rotating of facing. Air dried sand was pluviated from the slit of a hopper into a sand box. The height of hopper was kept always constant from the sand surface. The opening of slit and traveling speed of the hopper were carefully controlled so as to obtain a uniform sand layer of a constant dry unit weight γ_d with a thickness around 0.5 cm per one travel. After trimming the surface of top layer to the prescribed geometry, the whole sand box was tilted by 10 degrees except in case No.9 where no tilting was conducted, and the box was fixed at this position. Then the movable steel rod was pulled to rotate the facing at the toe. During these processes, forces acting on the facing and displacement of the facing were monitored.

The testing procedures using the large apparatus, where the facing was not connected to the sand box, are slightly different from those using the small apparatus. They consists of 2 steps: (1) filling of sand and (2) tilting of sand box, which were conducted in the same ways as for small apparatus.

In these pseudo-static test, the equivalent lateral seismic coefficient K_h can be defined as $K_h=tan\ \theta$, where θ is the tilting angle of sand box.

TEST RESULT AND DISCUSSIONS

Following figures show typical test results where Figs. 3~5 are for small apparatus, while Figs. 6~8 for large apparatus.

Fig. 3 shows measured force acting on the facing during filling of sand for small apparatus. The horizontal force measured by load cell Bp was larger than that measured by load cell A at the top. This indicates that the normal stress at the bottom part is larger than that at the upper part of the facing. The vertical force measured by load cell Bs also increases during filling of sand, which demonstrates that the facing of retaining wall is not perfectly smooth. As shown in Table 1, the measured coefficients of earth pressure at rest Ko were very close to $1-sin\ \phi$, where the value of shear resistance angle ϕ was evaluated based on the results of plane strain compression test conducted by Yoshida[10].

Fig. 4 shows measured forces acting on facing during tilting of sand box. The behavior of the horizontal forces measured by loads cell A and Bp were almost similar. This result may suggest that the pattern of normal stress

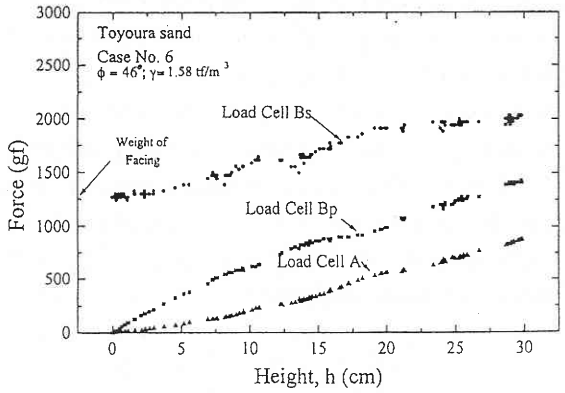

Fig. 3 Force in Load Cell During Filling of Sand for Small Apparatus

Table 1 Coefficient of Earth Pressure for Small Apparatus

CASE No.	CONDITION	K_o MEAS.	K_o 1-sin ϕ	K_a MEAS.	K_a $\tan^2(45-\phi/2)$	K_{ae} MEAS.	K_{ae} M-O(δ=0°)
5.	γ=1.58 tf/m^3 ϕ=46°; θ=10°	0.328	0.280	--	--	0.037	0.243
6.	γ=1.58 tf/m^3 ϕ=46°; θ=10°	0.310	0.280	--	--	0.077	0.243
8.	γ=1.49 tf/m^3 ϕ=45°; θ=10°	0.297	0.293	--	--	0.035	0.257
9.	γ=1.58 tf/m^3 ϕ=46°; θ=0°	0.272	0.280	0.035	0.163	--	--

M-O : Mononobe-Okabe Theory

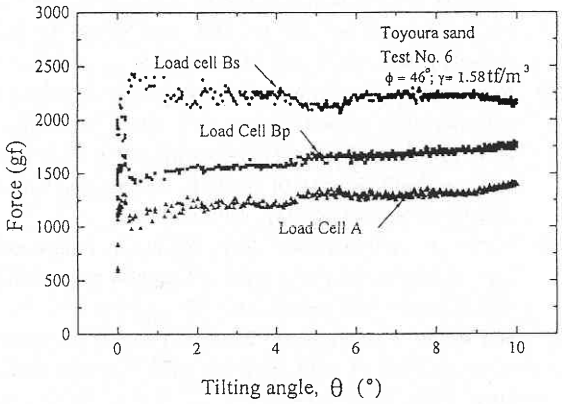

Fig. 4 Force in Load Cell During Tilting of Sand Box for Small Apparatus

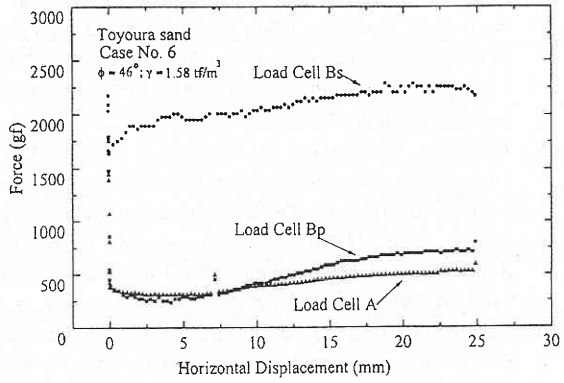

Fig. 5 Force in Load Cell vs. Displacement at the Top of Wall During Rotating of Facing for Small Apparatus

distribution does not change before and after the tilting.

Fig. 5 shows change of measured force during rotating of facing. The smallest horizontal force corresponding to the active earth pressure were observed at displacement at the top of facing around 3 mm. As shown in Table 1, the

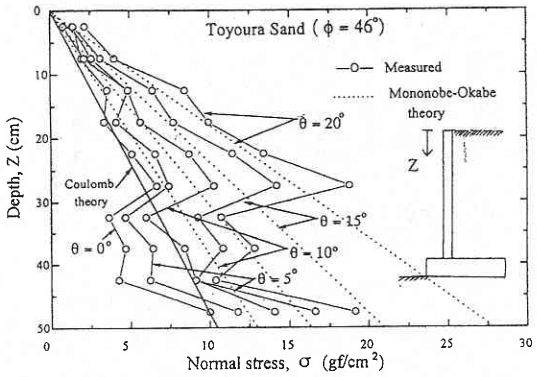

Fig. 6 Normal Stress Distribution on Backface of Facing During Tilting for Large Apparatus

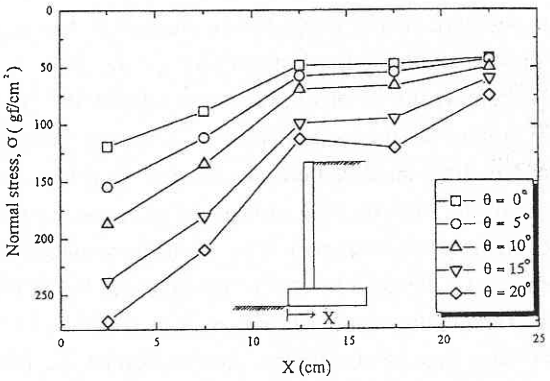

Fig. 7 Normal Stress Distribution on Bottom Side During Tilting for Large Apparatus

measured coefficients of active earth pressure K_{ae} were much smaller than those predicted by Mononobe-Okabe theory where the effect of friction between the facing and the back fill sand was ignored. This may be due to friction effect between sand and side walls for small apparatus.

Fig. 6 shows the normal horizontal stress distribution along the back face of facing for large apparatus. The measured earth pressure increased during tilting, the measured stress distributions were not triangular.

In the figure, also plotted is the earth pressure calculated based on Coulomb and Mononobe-Okabe theories for active earth pressure with ϕ=46° and δ=2/3 ϕ, where δ is the frictional angle between the facing and sand. The value of ϕ was obtained by plane stain compression tests referring to the same dry unit weight (1.58 tonf/m^3). It may be seen that for θ=0°~20°, the calculated and measured earth pressure are similar to each other for the upper two thirds of the facing, while the measured values are smaller at the

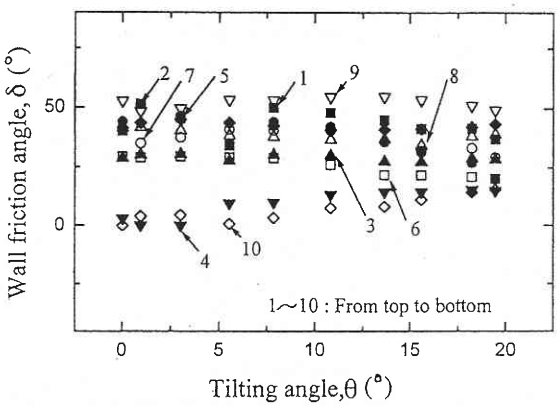

Fig. 8 Wall Friction Angle During Tilting for Large Apparatus

lower one third. This is likely due to effect of the friction on the upper surface of the bottom part of the wall.

Fig. 7 shows the normal vertical stress distribution along lower surface of the bottom part of retaining wall. The measured stress increased during tilting of sand box. Near the toe of the wall, the rate of increase of stress was much larger than at the other part. This result may suggest that the sand layer beneath the toe of the wall will fail at first.

Fig. 8 shows the measured friction angle $\delta = arctan\ (-\tau/\sigma)$ at the back face of the facing, plotted against the tilting angle θ. Although it was not constant along the facing, the values tend to converge to certain range after tilting.

SUMMARY of PRELIMINARY TEST

1. The measured horizontal forces acting on the back face of facing for small apparatus were much smaller compared with theoretical values, probably due to the effect of side wall friction, while the measured normal stresses acting on the back face of the facing were not very different from the theoretical value for large apparatus.
2. For large apparatus, the measured normal stress along the bottom of the wall increased during tilting, especially near the toe of the retaining wall, and the wall friction angle δ along the facing were not constant but tended to converge to some range.

Further investigation will be conducted by performing a series of model tests for different types of retaining walls by using large apparatus. (Manuscript received, April 30, 1996)

References

1) Mononobe, H., and Matsuo, H., On the Determination of Earth Pressures During Earthquakes, Proc. World Eng. Congress, 9, 1929.
2) Seed, H.B., and Whitman, R.V., Design of Earth Retaining Structure for Dynamic Loads, ASCE Specialty Conf. Lateral Stresses in the Ground and Design of Earth Retaining wall, 1970, pp. 103–147.
3) Newmark, N.M., Effects of earthquakes on dams and embankments, Geotechnique, 1965, 15(2), 139–161.
4) Richards, R., and Elms, D.G., Seismic behavior of gravity retaining walls, Journal of Geotech. Engineering Division, ASCE, 1979, Vol. 105(4), 449–465.
5) Nadim, F., and Whitman, R.V., Seimically induce movement of retaining walls, Journal of Geotech. Eng. Division, ASCE, 1983, Vol. 109(7), 915–931.
6) Sidharthan, R., and Norris, G.M., On the seismic displacement response of rigid retaining walls, Soil and Foundations, 1991, 31(2), 51–64.
7) Tatsuoka, F., Tateyama, M., Koseki, J., Performance of Soil Retaining walls for Railway Embankments, Special Issue of Soils and Foundations, Jan. 1996, 311–324.
8) Koseki, J., Tateyama, M., Tatsuoka, F., Horii, K., Preliminary Analysis of Soil Retaining Walls for Railway Embankments Damaged by The 1995 Hyogoken-Nambu Earthquake, Bulletin of Earthquake Resistant Structure Research Center, No.29, 1996, 65–77.
9) Tateyama, M., Murata, O., Tamura, Y., Nakamura, K., Tatsuoka, F., Nakaya, T., Lateral Loading test on columns on the facing of geosynthetic-reinforced soil retaining wall, Recent case Histories of Permanent Geosynthetic-Reinforced Soil Retaining walls, Ed. Tatsuoka and Leshinsky, Balkema 1994, 287–294.
10) Yoshida, T., Strain Localization and Shear Banding During Failure of Sands, Doctoral Thesis, University of Tokyo, 1995.